

Deficiency in I κ B α in the intestinal epithelium leads to spontaneous inflammation and mediates apoptosis in the gut

Nadine Mikuda^{1†}, Ruth Schmidt-Ullrich^{1†}, Eva Kärgel¹, Laura Golusda^{2,3}, Jana Wolf⁴, Uta E Höpken⁵, Claus Scheidereit¹, Anja A Kühl^{2,3} and Marina Kolesnichenko^{1*}

¹ Signal Transduction in Tumour Cells, Max Delbrück Centre for Molecular Medicine, Berlin, Germany

² Charité-Universitätsmedizin Berlin, Humboldt-Universität zu Berlin, Berlin, Germany

³ Berlin Institute of Health, iPATH.Berlin – Core Unit for Immunopathology, Berlin, Germany

⁴ Mathematical Modelling of Cellular Processes, Max Delbrück Centre for Molecular Medicine, Berlin, Germany

⁵ Microenvironmental Regulation in Autoimmunity and Cancer, Max Delbrück Centre for Molecular Medicine, Berlin, Germany

*Correspondence to: M Kolesnichenko, Signal Transduction in Tumour Cells, Max Delbrück Centre for Molecular Medicine, Robert-Rössle-Strasse 10, 13125 Berlin, Germany. E-mail: marina.k@oxfordalumni.org or marina.kolesnichenko@mdc-berlin.de

†These authors contributed equally to this work.

Abstract

The I κ B kinase (IKK)–NF- κ B signaling pathway plays a multifaceted role in inflammatory bowel disease (IBD): on the one hand, it protects from apoptosis; on the other, it activates transcription of numerous inflammatory cytokines and chemokines. Although several murine models of IBD rely on disruption of IKK–NF- κ B signaling, these involve either knockouts of a single family member of NF- κ B or of upstream kinases that are known to have additional, NF- κ B-independent, functions. This has made the distinct contribution of NF- κ B to homeostasis in intestinal epithelium cells difficult to assess. To examine the role of constitutive NF- κ B activation in intestinal epithelial cells, we generated a mouse model with a tissue-specific knockout of the direct inhibitor of NF- κ B, *Nfkb1a/I κ B α* . We demonstrate that constitutive activation of NF- κ B in intestinal epithelial cells induces several hallmarks of IBD including increased apoptosis, mucosal inflammation in both the small intestine and the colon, crypt hyperplasia, and depletion of Paneth cells, concomitant with aberrant Wnt signaling. To determine which NF- κ B-driven phenotypes are cell-intrinsic, and which are extrinsic and thus require the immune compartment, we established a long-term organoid culture. Constitutive NF- κ B promoted stem-cell proliferation, mis-localization of Paneth cells, and sensitization of intestinal epithelial cells to apoptosis in a cell-intrinsic manner. Increased number of stem cells was accompanied by a net increase in Wnt activity in organoids. Because aberrant Wnt signaling is associated with increased risk of cancer in IBD patients and because *NFKB1A* has recently emerged as a risk locus for IBD, our findings have critical implications for the clinic. In a context of constitutive NF- κ B, our findings imply that general anti-inflammatory or immunosuppressive therapies should be supplemented with direct targeting of NF- κ B within the epithelial compartment in order to attenuate apoptosis, inflammation, and hyperproliferation.

© 2020 The Authors. *The Journal of Pathology* published by John Wiley & Sons Ltd on behalf of Pathological Society of Great Britain and Ireland.

Keywords: inflammatory bowel disease; animal model; NF- κ B; precision medicine; inflammation; intestinal organoids; Wnt; stem cells; crypts

Received 26 October 2019; Revised 25 February 2020; Accepted 19 March 2020

No conflicts of interest were declared.

Introduction

IBD refers to autoimmune disorders, including ulcerative colitis (UC) and Crohn's disease (CD), which cause relapsing inflammation of the gastrointestinal tract [1,2]. Unlike in UC, where inflammation is mainly restricted to the colon and the rectum, in CD, the whole gastrointestinal tract can be affected, and the majority of patients present with terminal ileitis. Patients with IBD are at an increased risk of developing colorectal cancer later in life [3].

Hallmarks of IBD include an aberrant inflammatory response, increased apoptosis in intestinal epithelial cells (IECs), loss of epithelial barrier function, reduction in protective secretory Paneth cells, and dysbiosis [4–6].

Animal models have been indispensable in studying the pathology of inflammation in IBD [7,8]. The vast majority, however, have focused on disease pathogenesis in the colon and do not involve the small intestine (SI) [9]. Strikingly, a large fraction of genetically engineered murine models of IBD constitute knock-ins or

knockouts in the IKK–NF- κ B signaling pathway. NF- κ B plays a central role in IBD development and progression, and the level of activation of NF- κ B correlates with the severity of intestinal inflammation [10].

The transcription factor NF- κ B is composed of five distinct family members that form homo- and heterodimers that regulate diverse processes in the cell ranging from proliferation to inflammation, and apoptosis [11]. Stress stimuli, including bacterial toxins, inflammatory cytokines, and chemokines, and DNA damage converge on the upstream IKK complex, which activates NF- κ B by phosphorylating the inhibitor of the transcription factor, I κ B α , and thus targeting it for proteasomal degradation [12]. Liberated NF- κ B activates transcription of numerous target genes including inflammatory cytokines and chemokines but, importantly, also of *NFKBIA*, the gene coding for I κ B α [11]. Knockout of *Nfkb1a*/I κ B α in mice leads to early neonatal lethality, thereby posing an obstacle to studying the effect of activated NF- κ B in the mature gut [13,14]. Consequently, whether I κ B α knockout in the epithelial cells *in vivo*, and concomitant activation of NF- κ B, would lead to inflammation and immune cell response has remained unclear.

NF- κ B directly regulates the expression of numerous genes implicated in IBD pathogenesis, yet whether NF- κ B plays a pro- or an anti-inflammatory role in IECs has long been a matter of debate [10]. On the one hand, activation of NF- κ B leads to diverse inflammation-related pathologies [13–16], and direct inhibition of NF- κ B family member p65 abrogates established experimental colitis [17]. On the other hand, studies using IEC-specific knockout models that target kinases upstream of NF- κ B, specifically IKK γ , IKK β , and mitogen-activated protein kinase kinase kinase 7 (MAP3K7/TAK1), suggest that NF- κ B protects cells from apoptosis, thereby maintaining intestinal homeostasis [18–23]. These kinases, however, regulate additional signaling pathways apart from NF- κ B [12]. Indeed, we have recently shown that IKK represses activation of numerous inflammatory cytokines and chemokines independently of NF- κ B through destabilization of their mRNA [24]. Because different NF- κ B subunits can form functional heterodimers, knockouts of individual family members of NF- κ B do not directly address the role of the transcription factor in the pathogenesis of IBD. Therefore a murine model able to differentiate between contributions of IKK versus those of NF- κ B was still missing.

To determine which hallmarks of IBD are attributed to direct activation of NF- κ B and whether the transcription factor plays a pro- or an anti-apoptotic role in IECs, we generated mice with a specific I κ B α deletion in intestinal epithelial cells, *I κ B α ^{IEC-KO}*. We demonstrate that NF- κ B is constitutively activated in the intestinal epithelium of these mice, leading to expression of numerous inflammatory cytokines and chemokines. Surprisingly, despite activated NF- κ B, IECs of I κ B α -deficient mice were not protected from apoptosis and, on the contrary, were more sensitive to cytokine stimulation.

To dissect the cell-intrinsic from cell-extrinsic phenotypes, we cultured intestinal organoids. We demonstrate that the expression of pro-apoptotic genes and the net increased Wnt activity were a cell-intrinsic phenotype, associated with constitutive NF- κ B. Apoptosis and stem-cell identity in the crypt were mediated by extrinsic factors.

Materials and methods

Ethical issues

All aspects of animal care and experimental protocols in this study were approved by the regulatory standards of the Berlin Animal Review Board (LAGeSo Berlin) (Reg. G0082/13, G0358/13, G0092/18, G0111/19, and X9013/11).

Studies involving animals are reported in accordance with the ARRIVE guidelines [25,26].

Generation of *I κ B α ^{IEC-KO}* mice and preparation of mouse tissues from *in vivo* experiments

The generation of mice with floxed *Nfkb1a* (*I κ B α* gene) alleles (*B6*;129P2-*Nfkb1a*^{tm1Kbp}) has been described previously [27]. *I κ B α ^{IEC-KO}* mice were generated by mating *B6*;129P2-*Nfkb1a*^{tm1Kbp} with *Tg(Vil-cre)*20Syr (*Villin-cre*) mice [28]. Unless otherwise specified, the small intestine of mice between 8 and 15 weeks of age was used for experiments.

Scoring of inflammation in mice

Scoring was performed according to previously established guidelines [29].

RNA extraction

Small or large intestine was snap-frozen in liquid nitrogen and homogenized. RNA was extracted using Trizol reagent according to the manufacturer's instructions (Thermo Fisher Scientific, Waltham, MA, USA).

Western blot analysis and electrophoretic mobility shift assays (EMSA)

These were performed as described previously [24,30].

Immunofluorescence and IHC on paraffin tissue sections

Tissue sections were prepared as described previously [31,32]. Lists of antibodies and reagents may be found in supplementary material, Supplementary materials and methods. UEA-1(L8146; Sigma-Aldrich, St Louis, MO, USA) was prepared according to the manufacturer's instructions and used at 0.2 mg/ml final concentration according to the IHC protocol described previously [33].

Antibodies/primer sequences

These are given in supplementary material, Supplementary materials and methods.

Antibody array

The Proteome Profiler Antibody Array (R&D Systems, Minneapolis, MN, USA) was performed on 0.2 ml of serum according to the manufacturer's protocol. Quantification was performed with FusionCapt Advanced software.

RT-qPCR

This was carried out using a minimum of two reference genes (*Tbp1*, *Rpl13a*, *Hrpt1*, *Sdha*) according to the manufacturer's protocol (Promega, Madison, WI, USA).

Affymetrix array

Gene expression was measured with the mouse Clariom S Assay (Thermo Fisher Scientific) and analyzed using a Transcriptome Analysis Console 4.0. Further details are given in supplementary material, Supplementary materials and methods.

Preparation of organoids

Crypts were isolated from four to five mice per group as described elsewhere [34]. Organoids were grown for 12 days post-extraction. Immunofluorescence on organoids was performed as described elsewhere [35]. For RT-qPCR, 30–40 organoids were lysed in Trizol.

Gene set enrichment analysis (GSEA)

GSEA was performed as described in ref 36, using Molecular Signature Database v7.

Results

IκBα^{IEC-KO} mice develop spontaneous intestinal defects and inflammation

To investigate the impact of constitutive NF-κB signaling on the gut epithelium *in vivo*, we generated *IκBα*^{IEC-KO} mice lacking functional *IκBα* in the intestinal epithelium by crossing *IκBα*^{flox/flox} mice [27] with *Villin-cre* [28] transgenic mice (supplementary material, Figure S1A). Depletion of *IκBα* in the intestine was confirmed by western blot (Figure 1A and supplementary material, Figure S1B). *IκBα*^{IEC-KO} mice were born at normal Mendelian ratio and were phenotypically normal. However, from 7 weeks of age, *IκBα*^{IEC-KO} mice, but not littermate controls, presented with rectal prolapse, and by 42 weeks of age, 25% of the *IκBα*^{IEC-KO} mice were affected (Figure 1B). In addition, shorter colon, indicative of inflammation, and increased apoptosis were observed in *IκBα*^{IEC-KO} mice (Figures 1C–E). To determine if these mice developed spontaneous inflammation and morphological changes associated with colitis, we performed histomorphological scoring

as described previously [29]. Even in the absence of additional stimuli (e.g. DSS treatment), low-grade inflammation was detected in the colon (Figure 1F).

In the SI, premature, significantly enlarged Peyer's patches (PPs) were already visible in 4-week-old animals and became more prominent in adults (Figure 1G, H). A dramatic increase in size was accompanied by an increase in the B220 (CD45R)-positive B-lymphocyte compartment and the germinal center (Figure 1G and supplementary material, Figure S1C). From 8 weeks of age, *IκBα*^{IEC-KO} mice spontaneously developed mild intestinal inflammation (Figure 1I). Increase in infiltration by macrophages (F4/80⁺) and by T lymphocytes (CD3⁺) was confirmed by immunohistochemistry and quantified as described previously [29] (Figure 1J and supplementary material, Figure S1D).

Many cytokines that are upregulated in IBD are direct targets of NF-κB [37]. To determine if inflammation was systemic or confined to the intestine, we performed chemokine/cytokine array on the serum of *IκBα*^{IEC-KO} and control littermates (Figure 1K). We detected increased secretion of several mouse homologs of human markers of IBD, including metalloproteinase 3 (MMP3), platelet-derived growth factor (PDGF-BB), neutrophil gelatinase-associated lipocalin (LCN2/Ngal), macrophage colony-stimulating factor (CSF1/mCSF), and CC chemokine ligand 20 (CCL20) (Figure 1K). Because the above-mentioned targets are transcriptional targets of NF-κB (see the Gilmore database at <http://www.bu.edu/nf-kb/gene-resources/target-genes/>), we next sought to determine whether depletion of *IκBα* was sufficient to activate NF-κB and where this activation would take place.

Activated RelA/p65 in epithelium and in the follicle-associated epithelium (FAE) of *IκBα*^{IEC-KO} mice

Whole-body knockout (KO) of *Nfkb1a/IκBα* leads to neonatal lethality [13,14]. Nonetheless, increased DNA binding of NF-κB is only observed in some tissues and cells of *IκBα* KO neonates, such as granulocytes, which suggests that, in most tissues, knockout of *Nfkb1a/IκBα* alone is not sufficient for constitutive NF-κB activation [14]. To determine if absence of *IκBα* in the epithelium of the SI would lead to constitutive activation of NF-κB, we analyzed its DNA-binding activity and phosphorylation. NF-κB showed robust DNA-binding activity in *IκBα*^{IEC-KO} but in none of the control littermates (Figure 2A, top panel). To establish whether IKK contributed to activation of NF-κB, we analyzed phosphorylation of p65, a substrate of IKK. Only slight phosphorylation of p65 at S536 was detected. In contrast, in irradiated mouse embryonic fibroblasts (MEFs), strong phosphorylation of S536 was evident, and it was reduced in *Ikkβ* (IKKβ) knockout cells, as expected (Figure 2A, lower panel).

To determine where NF-κB was activated in IECs, we visualized translocation of the most prevalent subunit, p65, by immunofluorescence. Nuclear translocation of p65 was observed in villous epithelium of the *IκBα*^{IEC-KO} animals (Figure 2B). Similarly, we detected increased

production in the FAE of mutant mice (Figure 2C). To confirm that p65/NF-κB is activated, we analyzed expression of its bona-fide target genes: *Ccl20*, *Icam1*, *Tnf*, and *Tnfrsf25* (A20). All four

target genes were significantly upregulated (Figure 2D). In summary, we have demonstrated that epithelial knockout of *Nfkb1a/IκBα* is sufficient to activate NF-κB/p65 in IECs.

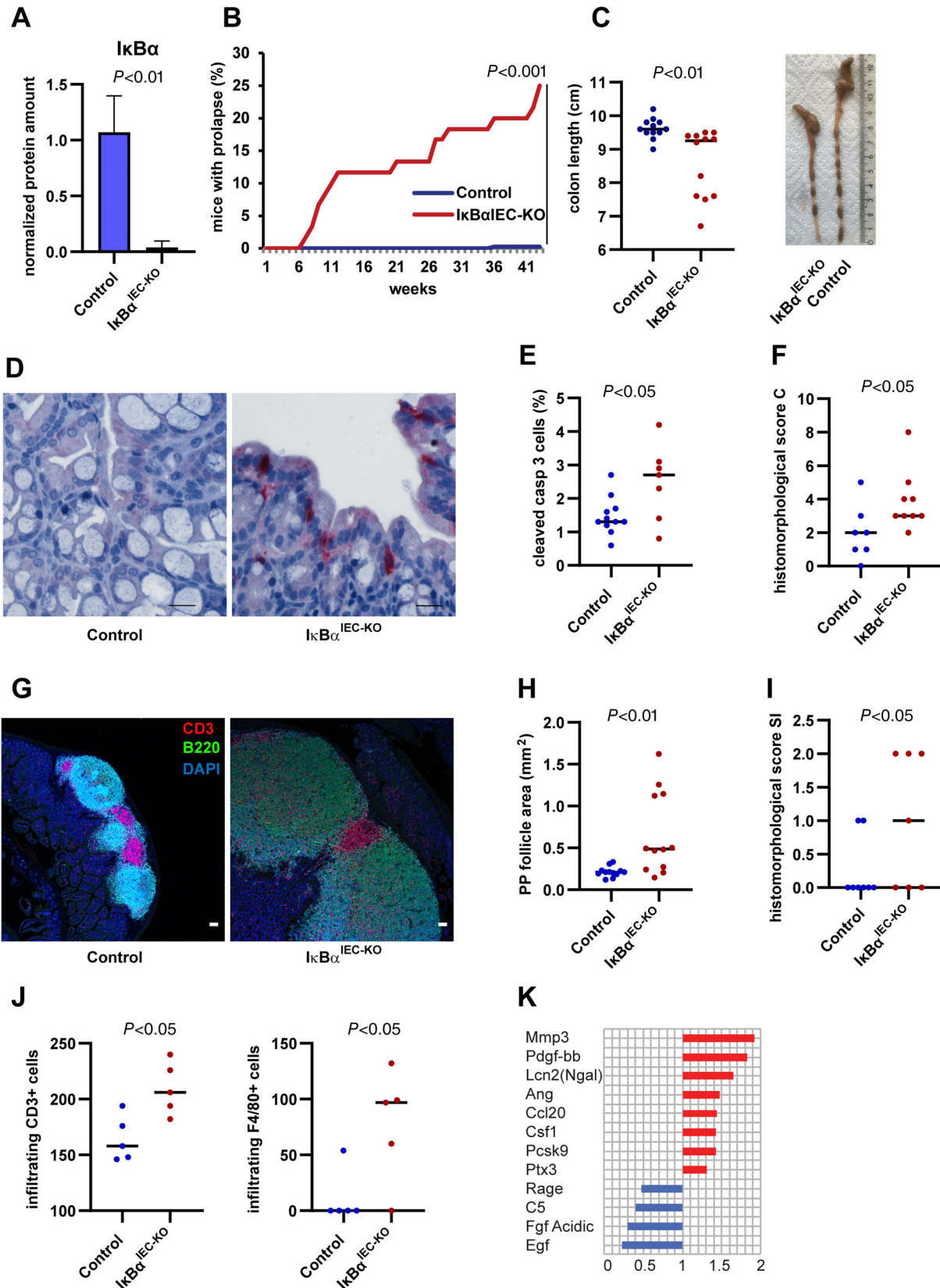


Figure 1 Legend on next page.

Constitutive NF- κ B mediates pro-apoptotic and pro-proliferative signaling in IECs

Since it was previously shown that NF- κ B protects against apoptosis, we performed microarray Affymetrix analysis on the SI of 8- to 11-week-old mice to determine whether deficiency of I κ B α and activation of p65 lead to anti-apoptotic gene expression as well as activation of biomarkers associated with IBD. We detected 116 downregulated transcripts, with a fold change of at least 2 between the I κ B α -deficient IECs and controls (Figure 3A). Expression of some members of the cytochrome P450 superfamily is significantly reduced in IBD, in part due to NF- κ B activation [38,39]. We detected 12 transcripts belonging to the cytochrome P450 superfamily (CYP3A, CYP2C, and CYP2J subfamilies) that showed a dramatic drop in expression in the intestines of the mutant mice (supplementary material, Table S1). Gene Ontology analysis revealed enrichment of downregulated genes in the categories of lipid catabolism, epoxygenase p450 pathway, and drug transport (Figure 3B), with the overarching category of metabolism. Surprisingly, lysozyme (*Lyz1*) and also other genes that are specific for Paneth cells [40], including mucosal pentraxin (*Mptx2*), colipase (*Clps*), and defensin alpha-related (*Defa-rs*), were downregulated in the I κ B α -deficient intestines (supplementary material, Table S1). Bulk analysis of the SI by microarray allowed us therefore to identify transcripts that were downregulated in *I κ B α ^{IEC-KO}* mice, and also to pinpoint which cells were likely affected.

We also detected 109 transcripts that showed a significant upregulation in IECs (Figure 3A and supplementary material, Table S1). Importantly, both key biomarkers of IBD, *Lcn2* and *Tnf*, appeared as the

highest upregulated transcripts in the small intestinal epithelium of *I κ B α ^{IEC-KO}* animals. Gene Ontology analysis showed enrichment for 'acute-phase response' and 'cellular response to tumor necrosis factor', with overarching term inflammation (Figure 3B). Surprisingly, none of the typical anti-apoptotic targets of NF- κ B, comprising the Bcl2 family members, appeared upregulated. In contrast, genes responsible for positive regulation of cell death and apoptosis, including interferon-induced protein with tetratricopeptide repeats 2 (*Ifit2*), NADPH oxidase (*Noxa*), and NADPH oxidase 1 (*Nox1*), were enriched (Figure 3C and supplementary material, Table S1). These data suggest that activation of NF- κ B resulting from deletion of *Nfkb1a*/I κ B α triggers a pro-apoptotic program in IECs and leads to upregulation of IBD-associated genes including *Lcn2*, *Tnf*, *Duox2*, and *Nos2*. GSEA revealed that in addition to NF- κ B, additional signaling pathways were activated (Figure 3D and supplementary material, Table S2). These included transcription factors, including Myc and E2F that regulate proliferation, and JAK-STAT3 and IFN γ signaling, which are associated with inflammatory response. Of note, pro-proliferative gene expression is distinct from the anti-apoptotic. The former implies increased cell duplication, whilst the latter indicates survival. We did not detect anti-apoptotic gene expression in *I κ B α ^{IEC-KO}* animals. Finally, analysis for associated diseases revealed the terms 'Ulcerative Colitis', 'Inflammatory Bowel Disease', and 'Crohn Disease', among others (supplementary material, Figure S2A,B).

Hyperplasia and Paneth cell loss in crypts

Paneth cells reside at the base of small-intestinal crypts, where they synthesize and secrete abundant quantities of

Figure 1. Abnormal intestinal development and spontaneous mild inflammation in *I κ B α ^{IEC-KO}*. (A) Whole cell lysates from four *I κ B α ^{IEC-KO}* mice and six littermate controls were analyzed by SDS-PAGE western blot. Protein expression was analyzed with Fusion Solo (Vilber Lourmat) and quantified (Fusion Capt V16.05a). Control was set to 1. A representative blot is shown in supplementary material, Figure S1B. Statistical significance was determined by Mann-Whitney *U*-test. Mean and SD are shown. (B) Incidence of rectal prolapse was recorded in *I κ B α ^{IEC-KO}* and control mice between 1 and 42 weeks of age. Significance was determined by chi-square test (two-sided) with Yates' correction. (C) Colon length in cm is shown. Two of the five mice with shorter colons also had prolapse. For C-F, mice were 32-42 weeks of age. Each point represents data from one animal and median is shown as a black bar. Example for length measurement is shown on the right. Lack of normal distribution in *I κ B α ^{IEC-KO}* colons was determined by Shapiro-Wilk test and statistical significance was measured by paired Wilcoxon test. (D) Representative images of immunohistochemistry showing cleaved caspase-3⁺ (red) cells in colon. Scale bars = 20 μ m. (E) Quantification of cleaved caspase-3⁺ epithelial cells in the colon. Points represent measurements (ten fields of vision with 100 cells per field) from individual animals in %. Statistical significance was determined by Mann-Whitney *U*-test. Median is shown. (F) Evaluation of histomorphology based on severity of mucosal infiltration, submucosal infiltration, and changes of crypt architecture. Scoring system for colon (C) inflammation: score from 0 to 12. Median is shown (black bar). Statistical significance was determined by Mann-Whitney *U*-test on *I κ B α ^{IEC-KO}* mice and their littermate controls. (G) Representative images of immunofluorescence (*n* = 5 per group) stain of PPs with DAPI⁺ nuclei (blue), B220/CD45R⁺ B cells (green), and CD3⁺ T cells (red). Scale bars = 50 μ m. (H) Area per follicle of PPs was quantified using ImageJ. PPs were quantified in small intestinal sections from *I κ B α ^{IEC-KO}* and control mice (> 8 weeks of age). Significance was calculated by Mann-Whitney *U*-test. (I) Histological inflammation score based on Erben *et al* [29]. Scoring system for small intestinal (SI) inflammation in consequence of cytokine imbalance. Score from 0 to 5, where 1 = mild inflammation (extent: mucosa), 2 = mild (mucosa and submucosa), 3 = moderate (mucosa and submucosa), 4 = marked (mucosa and submucosa and sometimes transmural), and 5 = marked with submucosal granuloma (mucosa, submucosa, transmural). Statistical significance was determined by paired Student's *t*-test; horizontal line represents the median (at 0 in controls). (J) Mean numbers of CD3⁺ T cells (left) and F4/80⁺ macrophages (right) within the mucosa of *I κ B α ^{IEC-KO}* and control mice. Positive cells were counted in ten high-power fields. Each point indicates average number per animal. Statistical significance was determined by paired Student's *t*-test; horizontal line represents the median (at 0 in controls). (K) ELISA-based antibody array (R&D Systems Large Mouse Antibody Array) was used to detect serum expression of cytokines in *I κ B α ^{IEC-KO}* and control mice (*n* = 4 per group). Cytokines showing significant differences between groups are shown in red for upregulated cytokines and in blue for downregulated expression. Significance was determined by Student's *t*-test. Horizontal axis shows fold change.

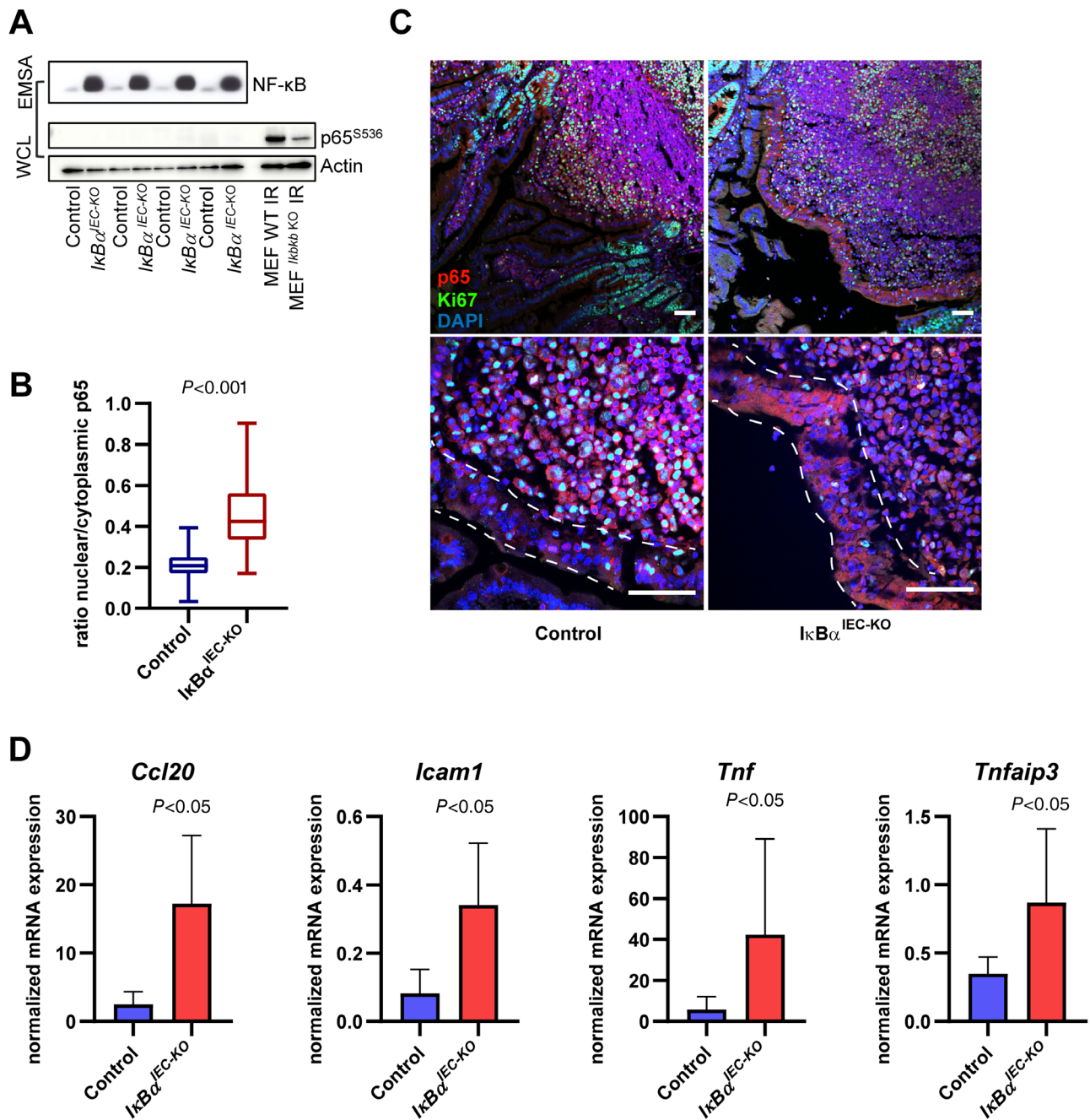


Figure 2. RelA (p65) is activated in IECs of $I\kappa B\alpha^{IEC-KO}$. (A) Electrophoretic mobility shift assay (EMSA) and SDS-PAGE performed on whole cell lysate (WCL) from bulk small intestine of littermate pairs ($n = 4$ per group). Top panel: EMSA shows DNA binding of NF- κ B in littermate pairs. SDS-PAGE western blot on the same lysates from above. As controls, irradiated wt and $I\kappa B\alpha$ KO (IKK β) MEFs (10 Gy) were harvested 1 h post-irradiation. (B) Graph shows quantification of nuclear p65 obtained by IF as a ratio (density) between nucleus/cytoplasm analyzed using ImageJ (version 2.0.0-rc.69/1.52n). Five mice per group and over six sections per mouse were analyzed. Whiskers indicate SD; significance was determined by Mann-Whitney U -test. (C) Representative images of IF of the small intestine, including PPs. The lines delineate FAE. Scale bars represent 50 μ m. Red: p65; green: Ki67; blue: DAPI. From $n = 5$ mice per group. Lower panels: higher magnification. (D) RNA from bulk small intestine was analyzed by RT-qPCR using primers for the genes shown. Expression was normalized to two reference genes. Significance was determined by Mann-Whitney U -test. Mean and SD are shown.

anti-microbial peptides and additionally help to sustain integrity of the intestinal epithelium [41,42]. Dysfunction of Paneth cells or loss through necroptosis or apoptosis contributes to the pathogenesis of IBD [43,44]. Since genes specific for Paneth cells were strongly downregulated in the SI of $I\kappa B\alpha^{IEC-KO}$ mice, we asked whether the cellular composition of

crypts was altered. Microscopic examination revealed hyperplasia in crypts and in the FAE (Figure 4A–C and supplementary material, Figure S3A). Paneth cells were depleted at crypt bases of the mutant animals (Figure 4D, E and supplementary material, Figures S3B–D). Some Paneth cells were mislocalized (Figure 4D, gray arrows), and crypt bases were instead occupied by Ki67⁺ cells.

However, no change in the number of goblet cells, another secretory cell type, was observed in the SI (supplementary material, Figure S3E). Depletion of Paneth

cells was further validated through loss of UEA-1 (*Ulex europaeus* agglutinin 1) that stains secretory granules (Figure 4F and supplementary material, Figure S3B

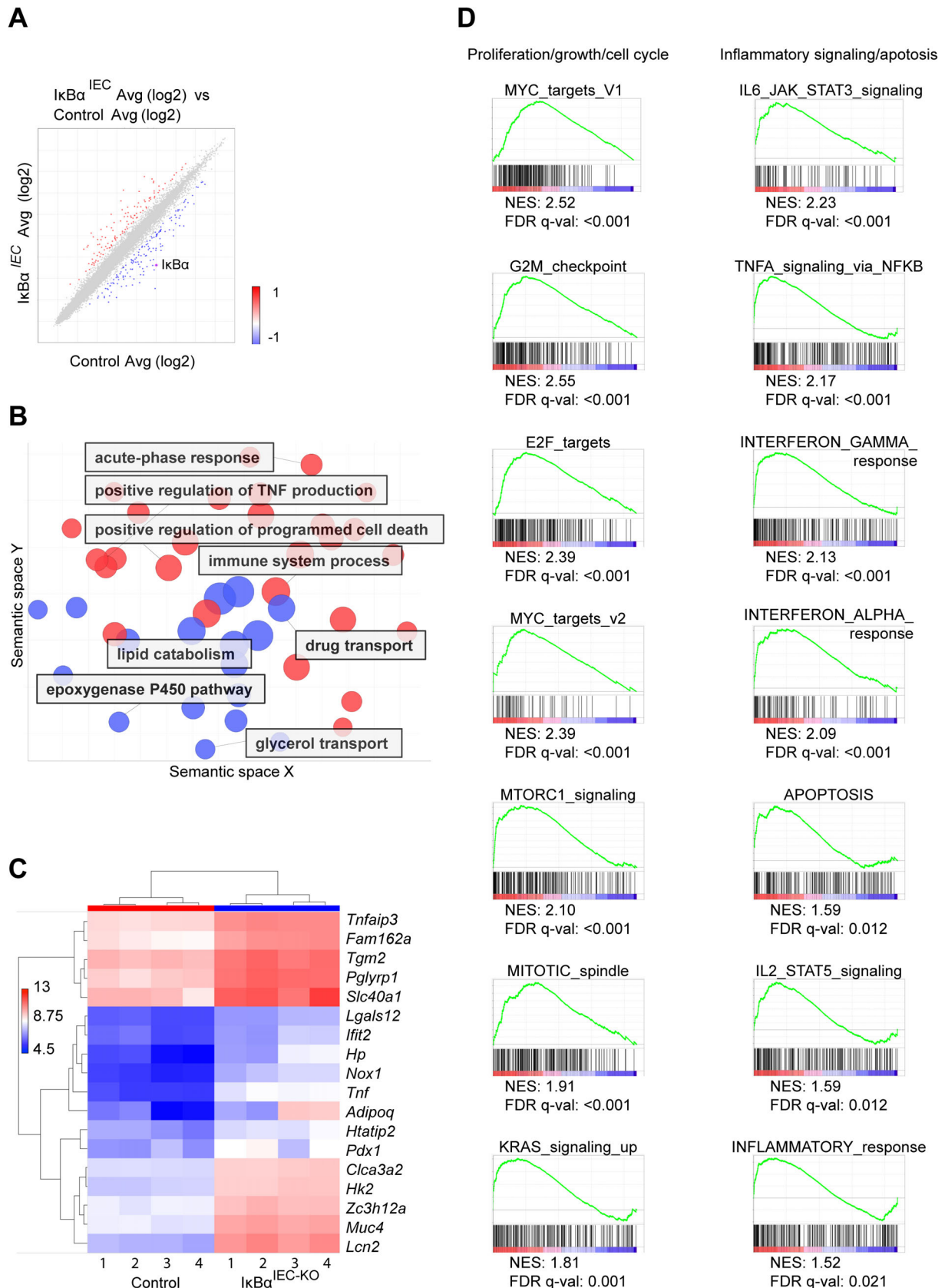


Figure 3 Legend on next page.

lower panels) and by staining for Sox9, which is also present in enteroendocrine cells, but at crypt bases is only in Paneth cells (supplementary material, Figure S3C). Paneth cells support stem-cell function by supplying essential factors [41]. Additionally, T helper cells were recently shown to mediate stem-cell differentiation [45–47]. A significantly lower number of Krt15⁺ stem cells per crypt were detected in *I κ B α ^{IEC-KO}* mice (Figure 4G,H). Krt15 is a marker for long-lived multipotent stem cells, whose expression is increased in *Lgr5*⁺ cells [48]. We confirmed reduced expression of *Lgr5* by RT-qPCR (Figure 4I). A recent single-cell survey of intestinal epithelium identified *Lgr5*⁺ and endothelin 1 (*Edn1*) as stem-cell specific markers for the least differentiated stem cells [intestinal stem cells (ISC)-I], and olfactomedin 4 (*Olfm4*) as a pan-stem cell marker [45]. We detected a significant drop in expression of *Edn1* but no significant change in *Olfm4* expression (supplementary material, Tables S1, S2, and Figure S3F,G). On the contrary, *Olfm4*⁺/*Ki67*⁺ stem cells extended into crypt bases (Figure 4J,K). Both *Lgr5* and *Edn1* are targets of Wnt signaling [49,50]. A decrease in the mRNA expression of certain Wnt targets detected by bulk analyses can, however, be indicative of loss of cell types expressing these and not of an overall effect of constitutive NF- κ B activation.

Constitutive NF- κ B results in aberrant Wnt activity in IECs

To determine which phenotypes resulting from constitutive NF- κ B are intrinsic versus extrinsic to IECs, we cultured small intestinal organoids. A significant proportion of organoids derived from *I κ B α ^{IEC-KO}* mice were either cystic or spheroid with enlarged crypts (Figure 5A–C and supplementary material, Figure S4A). This morphology is typically expected in a setting where Wnt signaling is activated [51], although a recent study showed that prolonged TNF α exposure can also lead to an appearance of spheroid or cystic organoids [52]. Yet, *in vivo*, we detected aberrant Wnt signaling: whereas some Wnt targets including *Myc*, *Nos2*, Frizzled homolog 7 (*Fzd7*), and *Cd44* were mildly upregulated, others, including *Lgr5* and *Edn1*, dropped in expression (Figure 4I and supplementary material, Table S3 and Figure S3F). As discussed above, this could be due to loss of cells driving Wnt or to extrinsic factors modulating expression of Wnt targets. There was no increase in

nuclear β -catenin (*Ctnnb1*) in these organoids (Figure 5A), unlike what is seen in APC-depleted cells [53]. Nevertheless, we did detect a significant increase in the expression of Wnt target genes, including *Axin2*, *Myc*, *Lgr5*, and *Sox9* (Figure 5D–F and supplementary material, Figure S4B). Expression of intestinal alkaline phosphatase, *Alpi*, a marker of enterocytes, was significantly decreased (Figure 5G). This indicates that constitutive NF- κ B signaling in organoids leads to an increase in *Lgr5*- and *Myc*-expressing cells at the expense of *Alpi*-expressing enterocytes.

To determine if Paneth cell loss of *I κ B α ^{IEC-KO}* mice was due to extrinsic or intrinsic factors, we stained intestinal organoids for *Lyz1*. In contrast to the *in vivo* setting, where clear loss of Paneth cells was observed in the *I κ B α* -deficient epithelium (Figure 4D–F), the *ex vivo* cultures harbored lysozyme-positive cells, albeit mostly in the lumen (Figure 5H). We then co-stained organoids for cleaved caspase-3 and β -galactosidase (β -gal). The latter is highly expressed in both secretory cell types (goblet and Paneth) in the mouse intestine (supplementary material, Figure S3D). β -Gal-positive cells localized exclusively to the lumen of *I κ B α* -deficient organoids, whereas in control animals many β -gal-positive cells could be seen in the budding crypts (supplementary material, Figure S4C). Epithelial turnover leads to shedding of cells into the lumen of organoids and, as expected, most cells that stained positive for the early apoptosis marker, cleaved caspase 3, were detected there (supplementary material, Figure S4C). Nevertheless, we did not detect an overall increase in double-positive (β -gal⁺ and cleaved caspase-3⁺) cells in *I κ B α* -deficient organoids. In summary, we have demonstrated that constitutive NF- κ B results in increased proliferation of stem cells, concomitant with a net increase in Wnt signaling, and mislocalization of Paneth cells. These phenotypes are intrinsic to IECs.

Hypersensitivity and apoptosis in *I κ B α* -deficient IECs after cytokine exposure

As shown above, the expression of several pro-apoptotic, but not anti-apoptotic, genes was significantly elevated in the SI of the *I κ B α ^{IEC-KO}* mice (Figure 3B–D and supplementary material, Table S1). Nonetheless, since we did not detect an increase in cells undergoing apoptosis in crypts of *I κ B α ^{IEC-KO}* mice (data not shown) or in untreated organoids from these animals

Figure 3. Pro-apoptotic gene signature in *I κ B α ^{IEC-KO}* mice. (A) RNA extracted from small intestines of mice ($n = 4$ per group) analyzed by Affymetrix microarray. Log₂ plot shows the distribution of significantly ($p < 0.05$) upregulated (red) and downregulated (blue) genes. *I κ B α* is highlighted by a pink circle. (B) Transcripts showing significant upregulation or downregulation analyzed by DAVID 6.8. Gene Ontology (GO) terms for up- and down-regulated transcripts (significance $p < 0.05$ Benjamini). GO terms were processed in REVIGO (semantic similarity setting Jiang & Conarth) to cluster related terms. The plot depicts GO terms associated with upregulated (red) and downregulated (blue) transcripts in *I κ B α ^{IEC-KO}* mice ($n = 4$) versus controls ($n = 4$). The X- and Y-axes show semantic space. Circle sizes represent log value prevalence. Proximities of circles to each other depict relationships between GO terms. (C) Heatmap showing expression of anti- and pro-apoptotic genes (DAVID 6.8 apoptosis, *Mus musculus*) in mouse pairs ($n = 4$ per group). The key shows expression levels. Genes with at least a two-fold change ($p < 0.05$) between two groups are shown. (D) GSEA was performed comparing the *I κ B α ^{IEC-KO}* gene list with the Molecular Signature Database v7. Enrichment plots for top hallmarks are shown. NES = normalized enrichment score; FDR = false discovery rate. Hallmarks grouped into two broad categories: proliferation/growth/cell cycle and inflammatory signaling/apoptosis.

(supplementary material, Figure S4C), we asked whether IκBα-deficient epithelial cells are more sensitive to stress. To this end, intestinal organoids from the

IκBα^{IEC-KO} mice and littermate controls were used to specifically examine the role of the pro-apoptotic contribution of NF-κB in the epithelium. As expected,

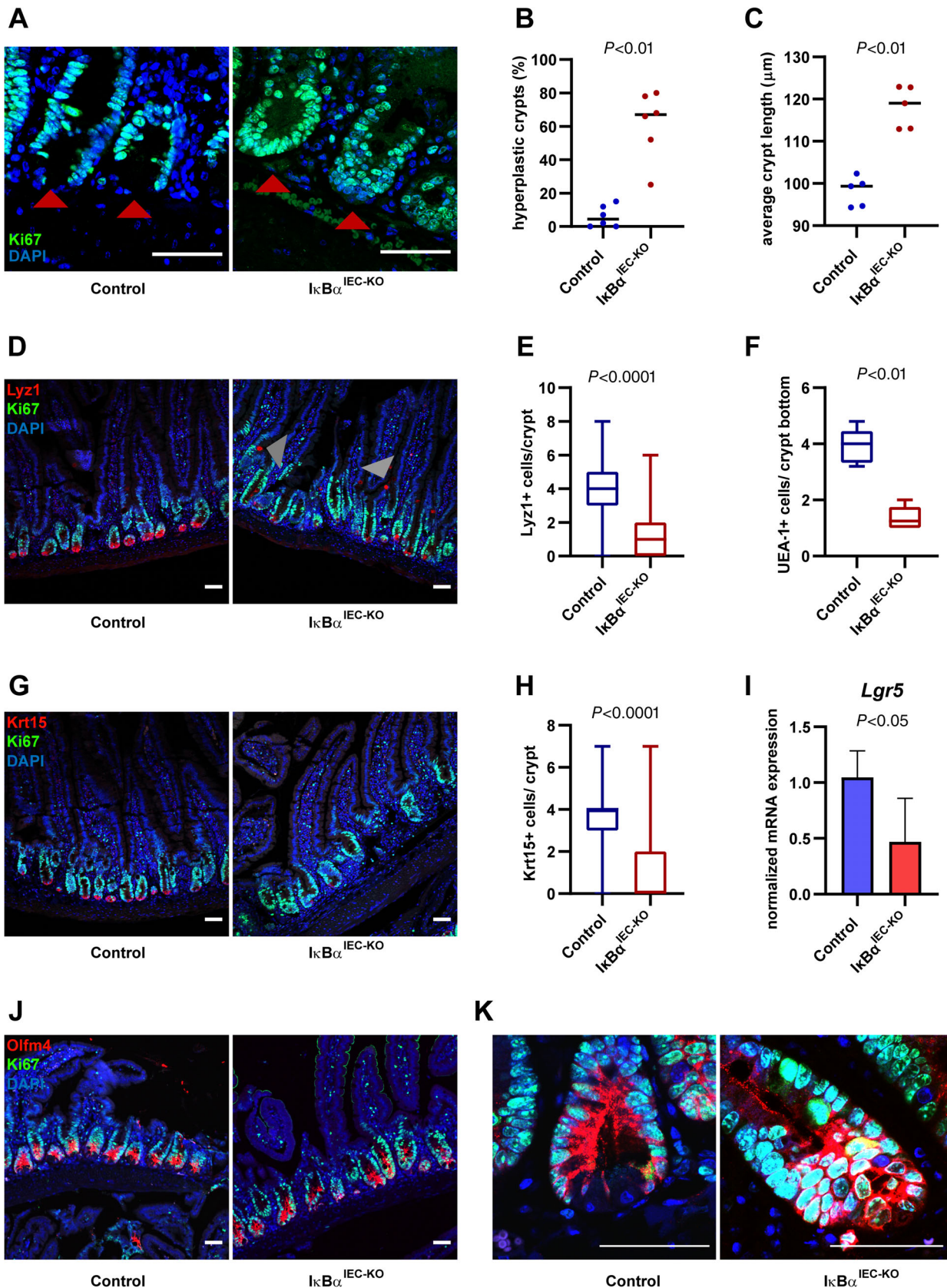


Figure 4 Legend on next page.

localization of cleaved caspase-3⁺ cells was restricted to the lumen in untreated organoids (Figure 6A, left panels). Treatment of intestinal organoids with sub-lethal doses of TNF α and INF γ resulted in a strong apoptotic response in the I κ B α -deficient organoids, but not in the controls (Figure 6A). In line with these data, we detected an upregulation of pro-apoptotic markers including *Tnf*, *Bax*, and *Noxa* (Figure 6B) in the I κ B α -deficient organoids (supplementary material, Figure S4D). These markers showed a further increase in expression following TNF α treatment. In summary, these data show that constitutive NF- κ B in IECs upregulates expression of pro-apoptotic and inflammatory genes through a cell-intrinsic mechanism, leading to an increased sensitivity to extrinsically mediated apoptosis.

Discussion

Whether NF- κ B plays a protective, anti-apoptotic role in IEC or drives inflammation and contributes to cell death remains controversial [10,13–15,18,19,21–23,43,54–56]. Furthermore, previous studies described knockouts of upstream kinases that could affect other signaling pathways, or of individual subunits, which may lead to compensatory upregulation of other NF- κ B family members [57]. To address these questions, we established mice with IEC-specific knockout of the direct inhibitor of NF- κ B, *Nfkb1a*/I κ B α . The mouse model displayed several hallmarks of IBD: inflammatory response, mucosal infiltration by CD3⁺ T cells and F4/80⁺ macrophages, serological markers associated with IBD, and expression of pro-inflammatory pro-apoptotic cytokines by IECs.

This mouse model does not encompass all aspects of IBD – ulceration, transmural infiltration, and acute inflammation were not detected. *I κ B α ^{IEC-KO}* mice displayed phenotypic variability in the degree of inflammatory response and associated expression of inflammatory cytokines, and also in the age of onset of rectal prolapse. We believe this is due to the dual role that I κ B α plays in regulation of NF- κ B: it both thwarts and terminates the response [14]. Here, we have shown that NF- κ B is activated even in the absence of an additional stimulus.

However, differential exposure to extrinsic stimuli in the environment would unleash a feed-forward loop of NF- κ B. This implies that the phenotype of *I κ B α ^{IEC-KO}* mice would worsen progressively with age, and that *I κ B α ^{IEC-KO}* mice would be especially sensitive to extrinsic stimuli.

Even in the absence of an additional stimulus, NF- κ B was constitutively activated in the I κ B α -deficient epithelium, and drove transcription of pro-apoptotic, but not of anti-apoptotic, genes. IECs underwent apoptosis in response to sub-lethal doses of cytokines.

Previous studies examining the contribution of NF- κ B to epithelial homeostasis discovered that tissue-specific knockout of the upstream activator IKK γ leads to the expression of inflammatory cytokines and also triggers apoptosis [19,58]. The anti-apoptotic role observed in this model may be due to an NF- κ B-independent role of IKK. IKK γ inhibits RIP kinase 1 (RIPK1) and can therefore protect IECs from apoptosis [58] in parallel or independently of NF- κ B. Overexpression of constitutively active *Ikkb*/IKK β [23,56] in part phenocopies *I κ B α ^{IEC-KO}*. The phenotype could be in part due to constitutive loss of I κ B α expression observed in cells expressing constitutively active *Ikkb*/IKK β [56]. It is possible that the protective role of NF- κ B stems from activation via IKK β , which is not the case in the epithelium of *I κ B α ^{IEC-KO}* mice. Guma *et al* also see hypersensitivity to TNF α in their model, and suggest that persistent activation of NF- κ B would upregulate pro-apoptotic functions and shift the balance towards cell death [56]. Our results provide experimental evidence for this hypothesis and reveal that, in the absence of activated IKK, NF- κ B alone plays a pro-apoptotic role in IECs.

In line with this, a study showing IEC-specific deletion of an indirect inhibitor of NF- κ B, *Tnfrsf25*/A20, [15] corroborates the pro-apoptotic role of NF- κ B in IECs. These IECs were hypersensitive to TNF α -induced apoptosis [15]. Unlike I κ B α , which directly sequesters NF- κ B in the cytoplasm, A20 functions at several junctions of the pathway, most notably by targeting upstream TRAF2 as well as IKK and RIP [59]. Deficiency of A20 in both the IECs and the myeloid cells leads to a similar phenotype observed in the present study [54].

Figure 4. Paneth cell loss accompanies crypt hyperplasia of *I κ B α ^{IEC-KO}* mice. (A) Representative image of IF of small intestine ($n = 7$ per group) showing Ki67⁺ proliferating cells (green). Nuclei were stained using DAPI (blue). Red arrows point to crypt bases. Scale bars represent 50 μ m. (B) Quantification of crypts showing abundance of Ki67⁺ cells at crypt bases. Points indicate average % of crypts with the phenotype per animal. Median is shown in black. Statistical significance was determined by Mann–Whitney *U*-test. (C) Average crypt length was measured using ImageJ. Points indicate average (based on 20–30 well-orientated crypts) length per mouse. (D) LYZ1⁺ Paneth cells (red) at the base of crypts in small intestinal sections in relation to Ki67⁺ proliferating cells (green); nuclei are stained using DAPI (blue). Scale bars = 50 μ m. Gray arrows point to mislocalized Paneth cells. (E) Mean/median \pm SD of LYZ1⁺ cells per crypt in more than 500 crypts per mouse ($n = 5$ per group). Statistical significance was determined by Mann–Whitney test. (F) UEA-1 cells at the bottom of 1/3 of crypts (25–30 crypts per mouse, with five mice per group) were counted. Statistical significance was determined by Mann–Whitney *U*-test. (G) Keratin 15 (KRT15)⁺ stem cells (red) in relation to Ki67⁺ proliferating cells (green) within the small intestine of *I κ B α ^{IEC-KO}* and control mice ($n = 6$ per group). Nuclei are stained with DAPI (blue). Scale bars = 50 μ m. (H) Krt15⁺ cells per crypt in *I κ B α ^{IEC-KO}* and control mice (with 30–40 crypts per mouse and $n = 6$ mice per group). (I) *Lgr5* expression analyzed by RT-qPCR from $n = 6$ mice per group. Mean and SD are shown. Statistical significance was determined by Mann–Whitney test. (J) Pan stem cell marker, Olfm4, positive stem cells (red) in relation to Ki67⁺ proliferating cells (green), within the small intestine of *I κ B α ^{IEC-KO}* and control mice ($n = 6$ per group). Scale bars = 50 μ m. (K) As in J but higher magnification, showing double Olfm4⁺/Ki67⁺-positive cells in crypt bases.

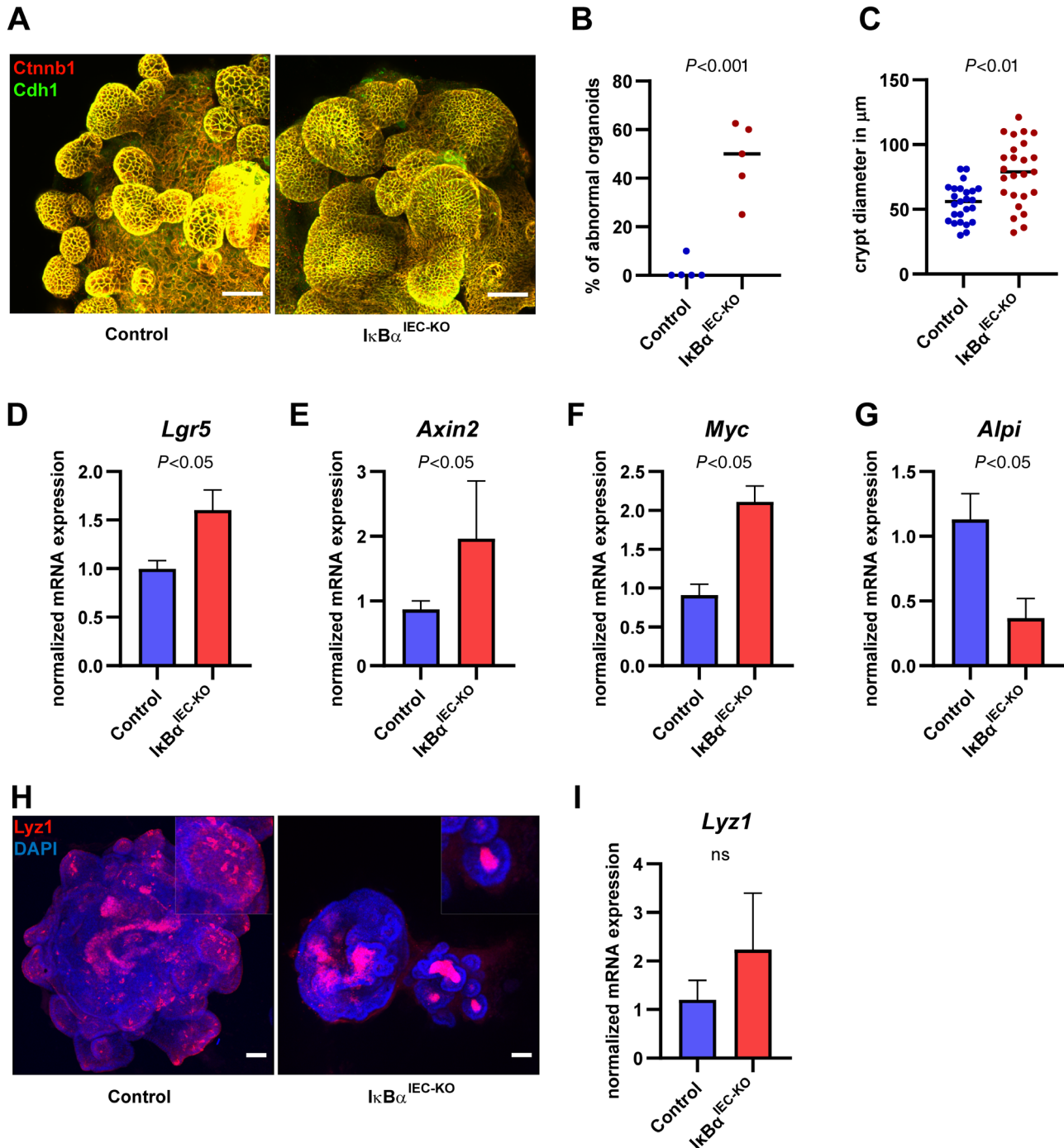


Figure 5. Intrinsic net positive regulation of Wnt by constitutive NF- κ B. (A) Small-intestinal organoids stained against active (non-phospho) β -catenin/Ctnnb1 (red) and E-cadherin/Cdh1 (green). Scale bars = 50 μ m. Representative images from a total of 20–25 organoids from $n = 4$ mice per group. (B) Percentage of abnormal (cystic or spheroid) organoids was calculated from over 20 organoids per mouse, with $n = 5$ mice per group. Statistical significance was determined by Mann–Whitney U -test. (C) Crypt diameter was measured in μ m. $n = 5$ mice per group. Statistical significance was determined by Mann–Whitney U -test. (D) RT–qPCR analysis of *Lgr5* RNA derived from organoids (from $n = 4$ mice per group). Expression was normalized to two reference genes. Statistical significance was determined by Student's t -test. Mean and SD are shown. (E) As in D showing *Axin2* expression. (F) As in D showing *Myc* expression. (G) As in D showing *Alpi* expression. (H) As in A stained with Lyz1 (red) and DAPI (blue). (I) As in D. ns = not significant.

In our mouse model, constitutive NF- κ B leads to an increase in transcription of its bona-fide targets, including that of *Tnfrsf25/A20*. Nevertheless, NF- κ B is decoupled from upstream signaling. Indeed, we would argue that persistent IKK–NF- κ B signaling that leads to constitutive depletion of I κ B α would ultimately result

in a subset of nuclear NF- κ B that is independent of A20 or IKK and thus lead to a partial overlap in phenotype with the *I κ B α ^{IEC-KO}* mice.

In parallel to pro-apoptotic signaling, we demonstrated that NF- κ B positively regulates proliferative response, in a cell-intrinsic manner. Hyperplastic crypts

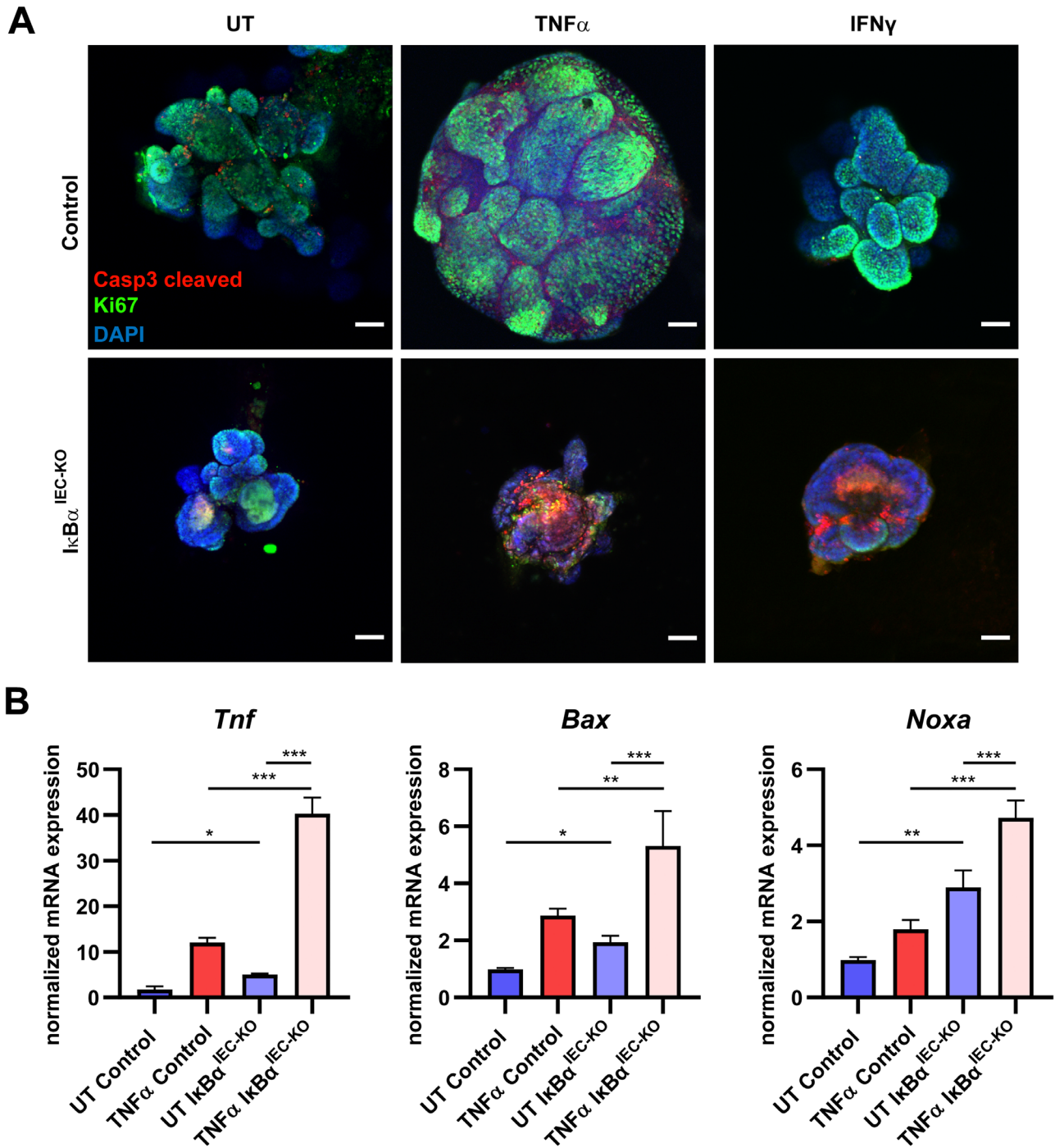


Figure 6. I κ B α -deficient IECs undergo cytokine-induced apoptosis. (A) Intestinal organoids from *I κ B α ^{IEC-KO}* and littermate controls (30–40 organoids from *n* = 3 mice per group) were treated with TNF α or IFN γ (10 ng/ml) or PBS as an untreated control (UT). After 16 h, organoids were analyzed by IF. Representative images from biological replicates (*n* = 5–10 organoids per condition, with *n* = 4 mice per group) show cleaved caspase-3⁺ apoptotic cells (red) and Ki67⁺ proliferating cells (green); nuclei are stained with DAPI (blue). Scale bars = 50 μ m. (B) RNA analyzed by RT-qPCR. Expression in control samples was set to 1. Variance was analyzed by one-way ANOVA. For *Bax*: *F* = 40.38, *Tnf*: *F* = 106.88, *Noxa*: *F* = 194.92. Tukey HSD *post hoc* test for all samples: *P* value between groups: **p* < 0.05; ***p* < 0.01; ****p* < 0.001.

were observed in mutant animals; however, ISC-I were less abundant.

Intestinal stem cells (ISCs) are the cells of origin for early neoplastic lesions [3,60,61]. The extent to which intrinsic factors, such as cell divisions of non-cancerous ISCs, contribute to cancer risk is a matter of debate [62,63]. Two recent studies have shown that an increase

in Lgr5⁺ cell number increases tumor susceptibility [64,65]. In both cases, an extrinsic factor (high fat diet) contributes to the phenotype [64,65]. An elegant recent study showed that a reduction of Lgr5⁺ cells accelerates tumorigenesis resulting from a reduction in competition between ISCs and a faster fixation of *Apc*-deficient cells [66]. Since neutral competition between stem cells

protects against accumulation of deleterious mutations, fixation of a single clone that contains oncogenic mutations can lead to tumorigenesis [66]. This is in line with the Goldilocks model that proposes that Wnt in a ‘just right’ amount, rather than its excessive activation, drives tumor formation [67,68]. Aberrant Wnt signaling is observed *in vivo* in our model, in part due to depletion of Paneth cells and altered composition of IECs. Aberrant Wnt signaling increases the probability of hitting the Goldilocks zone and therefore increases the risk of cancer development in IBD patients with constitutive NF- κ B activity in IECs.

Our findings are of great importance to the clinic. *NFKBIA* was identified as a risk locus for CD and a link between single nucleotide polymorphism in the 3' UTR of *NFKBIA* and IBD was discovered in at least some cohorts [69–71]. Notably, I κ B α protein is processed at a higher rate in the mucosa of CD patients, due to increased proteasomal degradation [72]. Our data imply that in the subset of patients with reduced levels of I κ B α , constitutively active NF- κ B would drive expression of a pro-proliferative and pro-apoptotic program in IECs. In addition, NF- κ B would lead to aberrant Wnt expression in crypts, increasing cancer risk for IBD patients. Consequently, constitutive NF- κ B activation in IECs is detrimental and therefore direct targeting of NF- κ B in IECs combined with anti-inflammatory approaches is likely to be more effective.

Acknowledgements

We are very grateful to Gabriele Born (Research Group ‘Genetics and Genomics of Cardiovascular Diseases’ AG Hübner, MDC) for Affymetrix chip hybridization and to Wolf-Hagen Schunck (MDC) for stimulating discussions. We would also like to thank Inge Krahn, Sabine Jungmann, Alexandra Schulze, Sarina Hilke, and Janine Wolff for excellent technical assistance; Sandra Cristina Carneiro Raimundo (Microscopy Facility, MDC); and Olga Kolesnichenko for help. And a big thank you to Daniela Keyner for keeping everything running smoothly. This work was supported in part by Deutsche Forschungsgemeinschaft (DFG) SCHE277/8-1, BMBF, CancerSys (ProSiTu) to CS; Deutsche Forschungsgemeinschaft (DFG) SFB1340 to LG and AAK, and TRR241 to AAK; and the Helmholtz-Gemeinschaft, Zukunftsthema ‘Immunology and Inflammation’ ZT-0027 to UEH.

Author contributions statement

MK designed the study. MK, NM, RSU, CS, AAK, UEH, and JW conceived the study. MK, NM, EK, and LG carried out experiments. AAK, EK, and MK performed formal data analysis. MK wrote the manuscript. MK, RSU, NM, EK, AAK, UEH, and LG edited the manuscript. CS, AAK, and UEH acquired funding.

References

- Torres J, Mehandru S, Colombel JF, et al. Crohn's disease. *Lancet* 2017; **389**: 1741–1755.
- Thorsteinsdottir S, Gudjonsson T, Nielsen OH, et al. Pathogenesis and biomarkers of carcinogenesis in ulcerative colitis. *Nat Rev Gastroenterol Hepatol* 2011; **8**: 395–404.
- Spit M, Koo BK, Maurice MM. Tales from the crypt: intestinal niche signals in tissue renewal, plasticity and cancer. *Open Biol* 2018; **8**: 180120.
- Martini E, Krug SM, Siegmund B, et al. Mend your fences: the epithelial barrier and its relationship with mucosal immunity in inflammatory bowel disease. *Cell Mol Gastroenterol Hepatol* 2017; **4**: 33–46.
- Xavier RJ, Podolsky DK. Unravelling the pathogenesis of inflammatory bowel disease. *Nature* 2007; **448**: 427–434.
- Nunes T, Bernardazzi C, de Souza HS. Cell death and inflammatory bowel diseases: apoptosis, necrosis, and autophagy in the intestinal epithelium. *Biomed Res Int* 2014; **2014**: 218493.
- Mizoguchi A, Takeuchi T, Himuro H, et al. Genetically engineered mouse models for studying inflammatory bowel disease. *J Pathol* 2016; **238**: 205–219.
- Wirtz S, Popp V, Kindermann M, et al. Chemically induced mouse models of acute and chronic intestinal inflammation. *Nat Protoc* 2017; **12**: 1295–1309.
- Pizarro TT, Arseneau KO, Bamias G, et al. Mouse models for the study of Crohn's disease. *Trends Mol Med* 2003; **9**: 218–222.
- Atreya I, Atreya R, Neurath MF. NF-kappaB in inflammatory bowel disease. *J Intern Med* 2008; **263**: 591–596.
- Zhang Q, Lenardo MJ, Baltimore D. 30 years of NF- κ B: a blossoming of relevance to human pathobiology. *Cell* 2017; **168**: 37–57.
- Hinz M, Scheidereit C. The I κ B kinase complex in NF- κ B regulation and beyond. *EMBO Rep* 2014; **15**: 46–61.
- Klement JF, Rice NR, Car BD, et al. I κ B α deficiency results in a sustained NF- κ B response and severe widespread dermatitis in mice. *Mol Cell Biol* 1996; **16**: 2341–2349.
- Beg AA, Sha WC, Bronson RT, et al. Constitutive NF- κ B activation, enhanced granulopoiesis, and neonatal lethality in I κ B α -deficient mice. *Genes Dev* 1995; **9**: 2736–2746.
- Vereecke L, Sze M, Mc Guire C, et al. Enterocyte-specific A20 deficiency sensitizes to tumor necrosis factor-induced toxicity and experimental colitis. *J Exp Med* 2010; **207**: 1513–1523.
- Kondylis V, Kumari S, Vlantis K, et al. The interplay of IKK, NF- κ B and RIPK1 signaling in the regulation of cell death, tissue homeostasis and inflammation. *Immunol Rev* 2017; **277**: 113–127.
- Neurath MF, Pettersson S, Meyer zum Buschenfelde KH, et al. Local administration of antisense phosphorothioate oligonucleotides to the p65 subunit of NF- κ B abrogates established experimental colitis in mice. *Nat Med* 1996; **2**: 998–1004.
- Kajino-Sakamoto R, Inagaki M, Lippert E, et al. Enterocyte-derived TAK1 signaling prevents epithelium apoptosis and the development of ileitis and colitis. *J Immunol* 2008; **181**: 1143–1152.
- Nenci A, Becker C, Wullaert A, et al. Epithelial NEMO links innate immunity to chronic intestinal inflammation. *Nature* 2007; **446**: 557–561.
- Greten FR, Eckmann L, Greten TF, et al. IKK β links inflammation and tumorigenesis in a mouse model of colitis-associated cancer. *Cell* 2004; **118**: 285–296.
- Eckmann L, Nebelsiek T, Fingerle AA, et al. Opposing functions of IKK β during acute and chronic intestinal inflammation. *Proc Natl Acad Sci U S A* 2008; **105**: 15058–15063.
- Zaph C, Troy AE, Taylor BC, et al. Epithelial-cell-intrinsic IKK- β expression regulates intestinal immune homeostasis. *Nature* 2007; **446**: 552–556.

23. Vlantis K, Wullaert A, Sasaki Y, *et al.* Constitutive IKK2 activation in intestinal epithelial cells induces intestinal tumors in mice. *J Clin Invest* 2011; **121**: 2781–2793.
24. Mikuda N, Kolesnichenko M, Beaudette P, *et al.* The I κ B kinase complex is a regulator of mRNA stability. *EMBO J* 2018; **14**: 24.
25. McGrath JC, Drummond GB, McLachlan EM, *et al.* Guidelines for reporting experiments involving animals: the ARRIVE guidelines. *Br J Pharmacol* 2010; **160**: 1573–1576.
26. Kilkenny C, Browne WJ, Cuthill IC, *et al.* Improving bioscience research reporting: the ARRIVE guidelines for reporting animal research. *PLoS Biol* 2010; **8**: e1000412.
27. Rupec RA, Jundt F, Rebholz B, *et al.* Stroma-mediated dysregulation of myelopoiesis in mice lacking I κ B α . *Immunity* 2005; **22**: 479–491.
28. el Marjou F, Janssen KP, Chang BH, *et al.* Tissue-specific and inducible Cre-mediated recombination in the gut epithelium. *Genesis* 2004; **39**: 186–193.
29. Erben U, Lodenkemper C, Doerfel K, *et al.* A guide to histomorphological evaluation of intestinal inflammation in mouse models. *Int J Clin Exp Pathol* 2014; **7**: 4557–4576.
30. Kolesnichenko M, Hong L, Liao R, *et al.* Attenuation of TORC1 signaling delays replicative and oncogenic RAS-induced senescence. *Cell Cycle* 2012; **11**: 2391–2401.
31. Krieger K, Millar SE, Mikuda N, *et al.* NF- κ B participates in mouse hair cycle control and plays distinct roles in the various pelage hair follicle types. *J Invest Dermatol* 2018; **138**: 256–264.
32. Zhang Y, Tomann P, Andl T, *et al.* Reciprocal requirements for EDA/EDAR/NF- κ B and Wnt/ β -catenin signaling pathways in hair follicle induction. *Dev Cell* 2009; **17**: 49–61.
33. Wichner K, Stauss D, Kampfrath B, *et al.* Dysregulated development of IL-17- and IL-21-expressing follicular helper T cells and increased germinal center formation in the absence of ROR γ t. *FASEB J* 2016; **30**: 761–774.
34. Sato T, Stange DE, Ferrante M, *et al.* Long-term expansion of epithelial organoids from human colon, adenoma, adenocarcinoma, and Barrett's epithelium. *Gastroenterology* 2011; **141**: 1762–1772.
35. O'Rourke KP, Dow LE, Lowe SW. Immunofluorescent staining of mouse intestinal stem cells. *Bio Protoc* 2016; **6**: e1732.
36. Subramanian A, Tamayo P, Mootha VK, *et al.* Gene set enrichment analysis: a knowledge-based approach for interpreting genome-wide expression profiles. *Proc Natl Acad Sci U S A* 2005; **102**: 15545–15550.
37. Neurath MF. Cytokines in inflammatory bowel disease. *Nat Rev Immunol* 2014; **14**: 329–342.
38. Zordoky BN, El-Kadi AO. Role of NF- κ B in the regulation of cytochrome P450 enzymes. *Curr Drug Metab* 2009; **10**: 164–178.
39. Morgan ET. Impact of infectious and inflammatory disease on cytochrome P450-mediated drug metabolism and pharmacokinetics. *Clin Pharmacol Ther* 2009; **85**: 434–438.
40. Haber AL, Biton M, Rogel N, *et al.* A single-cell survey of the small intestinal epithelium. *Nature* 2017; **551**: 333–339.
41. Clevers HC, Bevins CL. Paneth cells: maestros of the small intestinal crypts. *Annu Rev Physiol* 2013; **75**: 289–311.
42. Stappenbeck TS. Paneth cell development, differentiation, and function: new molecular cues. *Gastroenterology* 2009; **137**: 30–33.
43. Dannappel M, Vlantis K, Kumari S, *et al.* RIPK1 maintains epithelial homeostasis by inhibiting apoptosis and necroptosis. *Nature* 2014; **513**: 90–94.
44. Farin HF, Karthaus WR, Kujala P, *et al.* Paneth cell extrusion and release of antimicrobial products is directly controlled by immune cell-derived IFN- γ . *J Exp Med* 2014; **211**: 1393–1405.
45. Biton M, Haber AL, Rogel N, *et al.* T helper cell cytokines modulate intestinal stem cell renewal and differentiation. *Cell* 2018; **175**: 1307–1320 e1322.
46. Lindemans CA, Calafiore M, Mertelsmann AM, *et al.* Interleukin-22 promotes intestinal-stem-cell-mediated epithelial regeneration. *Nature* 2015; **528**: 560–564.
47. Naik S, Larsen SB, Cowley CJ, *et al.* Two to tango: dialog between immunity and stem cells in health and disease. *Cell* 2018; **175**: 908–920.
48. Giroux V, Stephan J, Chatterji P, *et al.* Mouse intestinal Krt15+ crypt cells are radio-resistant and tumor initiating. *Stem Cell Reports* 2018; **10**: 1947–1958.
49. Barker N, van Es JH, Kuipers J, *et al.* Identification of stem cells in small intestine and colon by marker gene Lgr5. *Nature* 2007; **449**: 1003–1007.
50. Kim TH, Xiong H, Zhang Z, *et al.* Beta-catenin activates the growth factor endothelin-1 in colon cancer cells. *Oncogene* 2005; **24**: 597–604.
51. Merenda A, Fenderico N, Maurice MM. Wnt signaling in 3D: recent advances in the applications of intestinal organoids. *Trends Cell Biol* 2020; **30**: 60–73.
52. Hahn S, Nam MO, Noh JH, *et al.* Organoid-based epithelial to mesenchymal transition (OEMT) model: from an intestinal fibrosis perspective. *Sci Rep* 2017; **7**: 2435.
53. Gregorieff A, Clevers H. Wnt signaling in the intestinal epithelium: from endoderm to cancer. *Genes Dev* 2005; **19**: 877–890.
54. Vereecke L, Vieira-Silva S, Billiet T, *et al.* A20 controls intestinal homeostasis through cell-specific activities. *Nat Commun* 2014; **5**: 5103.
55. Kontoyiannis D, Pasparakis M, Pizarro TT, *et al.* Impaired on/off regulation of TNF biosynthesis in mice lacking TNF AU-rich elements: implications for joint and gut-associated immunopathologies. *Immunity* 1999; **10**: 387–398.
56. Guma M, Stepniak D, Shaked H, *et al.* Constitutive intestinal NF- κ B does not trigger destructive inflammation unless accompanied by MAPK activation. *J Exp Med* 2011; **208**: 1889–1900.
57. Steinbrecher KA, Harmel-Laws E, Sitcheran R, *et al.* Loss of epithelial RelA results in deregulated intestinal proliferative/apoptotic homeostasis and susceptibility to inflammation. *J Immunol* 2008; **180**: 2588–2599.
58. Vlantis K, Wullaert A, Polykratis A, *et al.* NEMO prevents RIP kinase 1-mediated epithelial cell death and chronic intestinal inflammation by NF- κ B-dependent and -independent functions. *Immunity* 2016; **44**: 553–567.
59. Shembade N, Harhaj EW. Regulation of NF- κ B signaling by the A20 deubiquitinase. *Cell Mol Immunol* 2012; **9**: 123–130.
60. Fevr T, Robine S, Louvard D, *et al.* Wnt/ β -catenin is essential for intestinal homeostasis and maintenance of intestinal stem cells. *Mol Cell Biol* 2007; **27**: 7551–7559.
61. Barker N, Ridgway RA, van Es JH, *et al.* Crypt stem cells as the cells-of-origin of intestinal cancer. *Nature* 2009; **457**: 608–611.
62. Wu S, Powers S, Zhu W, *et al.* Substantial contribution of extrinsic risk factors to cancer development. *Nature* 2016; **529**: 43–47.
63. Tomasetti C, Vogelstein B. Cancer etiology. Variation in cancer risk among tissues can be explained by the number of stem cell divisions. *Science* 2015; **347**: 78–81.
64. Beyaz S, Mana MD, Roper J, *et al.* High-fat diet enhances stemness and tumorigenicity of intestinal progenitors. *Nature* 2016; **531**: 53–58.
65. Fu T, Coulter S, Yoshihara E, *et al.* FXR regulates intestinal cancer stem cell proliferation. *Cell* 2019; **176**: 1098–1112 e1018.
66. Huels DJ, Bruens L, Hodder MC, *et al.* Wnt ligands influence tumour initiation by controlling the number of intestinal stem cells. *Nat Commun* 2018; **9**: 1132.

67. Albuquerque C, Breukel C, van der Luijt R, *et al.* The 'just-right' signaling model: APC somatic mutations are selected based on a specific level of activation of the β -catenin signaling cascade. *Hum Mol Genet* 2002; **11**: 1549–1560.
68. Flanagan DJ, Austin CR, Vincan E, *et al.* Wnt signalling in gastrointestinal epithelial stem cells. *Genes* 2018; **9**: 178.
69. Hong SN, Park C, Park SJ, *et al.* Deep resequencing of 131 Crohn's disease associated genes in pooled DNA confirmed three reported variants and identified eight novel variants. *Gut* 2016; **65**: 788–796.
70. Szamosi T, Lakatos PL, Szilvasi A, *et al.* The 3'UTR NFKBIA variant is associated with extensive colitis in Hungarian IBD patients. *Dig Dis Sci* 2009; **54**: 351–359.
71. Klein W, Tromm A, Folwaczny C, *et al.* A polymorphism of the NFKBIA gene is associated with Crohn's disease patients lacking a predisposing allele of the CARD15 gene. *Int J Colorectal Dis* 2004; **19**: 153–156.
72. Visekruna A, Joeris T, Seidel D, *et al.* Proteasome-mediated degradation of I κ B α and processing of p105 in Crohn disease and ulcerative colitis. *J Clin Invest* 2006; **116**: 3195–3203.
- *73. Piñero J, Queralt-Rosinach N, Bravo A, *et al.* DisGeNET: a discovery platform for the dynamical exploration of human diseases and their genes. *Database* 2015; **2015**: bav028.
- *Cited only in supplementary material.

SUPPLEMENTARY MATERIAL ONLINE

Supplementary materials and methods

Supplementary figure legends

Supplementary table legends

Figure S1. Intestinal abnormalities observed in *I κ B α ^{IEC-KO}* mice

Figure S2. Disease signatures associated with the *I κ B α ^{IEC-KO}* gene set

Figure S3. Altered crypt cell composition in *I κ B α ^{IEC-KO}* mice

Figure S4. Mislocalization of Paneth cells and net increase in Wnt activity in organoids from *I κ B α ^{IEC-KO}* mice

Table S1. Gene expression in *I κ B α ^{IEC-KO}* mice

Table S2. Gene set enrichment analysis (GSEA) hallmarks

Table S3. Wnt targets regulated in *I κ B α ^{IEC-KO}* mice

25 Years ago in *The Journal of Pathology*...

Accumulation of p53 protein in normal, dysplastic, and neoplastic Barrett's oesophagus

Kausilia K. Krishnadath, Hugo W. Tilanus, Mark van Blankenstein, Fre T. Bosman, Andries H. Mulder

p53 expression in normal, dysplastic, and neoplastic laryngeal epithelium. Absence of a correlation with prognostic factors

Alfons Nadal, Elías Campo, José Pinto, Carme Mallofré, Antonio Palacín, Carlos Arias, José Traserra, Antonio Cardesa

PCR-mismatch analysis of p53 gene mutation in Hodgkin's disease

Luc Xerri, Patricia Parc, Reda Bouabdallah, Jacques Camerlo, Jacques Hassoun

To view these articles, and more, please visit:

www.thejournalofpathology.com

Click 'BROWSE' and select 'All issues', to read articles going right back to Volume 1, Issue 1 published in 1892.

The Journal of Pathology
Understanding Disease

